

Accepted Manuscript

Surrogating and redirection of Pyrazolo[1,5-a]pyrimidin-7(4H)-one core, a novel class of potent and selective DPP-4 Inhibitors

Xinxian Deng, Jian Shen, Hui Zhu, Jia Xiao, Ran Sun, Fangzhou Xie, Celine Lam, Juntao Wang, Yixue Qiao, Mojdeh S. Tavallaie, Yang Hu, Yi Du, Jianqi Li, Lei Fu, Faqin Jiang

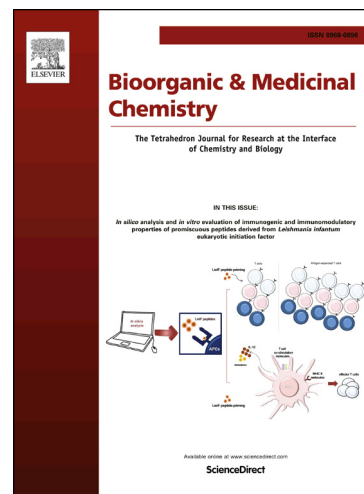
PII: S0968-0896(17)32286-1
DOI: <https://doi.org/10.1016/j.bmc.2018.01.006>
Reference: BMC 14160

To appear in: *Bioorganic & Medicinal Chemistry*

Received Date: 23 November 2017
Revised Date: 9 January 2018
Accepted Date: 10 January 2018

Please cite this article as: Deng, X., Shen, J., Zhu, H., Xiao, J., Sun, R., Xie, F., Lam, C., Wang, J., Qiao, Y., Tavallaie, M.S., Hu, Y., Du, Y., Li, J., Fu, L., Jiang, F., Surrogating and redirection of Pyrazolo[1,5-a]pyrimidin-7(4H)-one core, a novel class of potent and selective DPP-4 Inhibitors, *Bioorganic & Medicinal Chemistry* (2018), doi: <https://doi.org/10.1016/j.bmc.2018.01.006>

This is a PDF file of an unedited manuscript that has been accepted for publication. As a service to our customers we are providing this early version of the manuscript. The manuscript will undergo copyediting, typesetting, and review of the resulting proof before it is published in its final form. Please note that during the production process errors may be discovered which could affect the content, and all legal disclaimers that apply to the journal pertain.



Surrogating and redirection of Pyrazolo[1,5-a]pyrimidin-7(4H)-one core, a novel class of potent and selective DPP-4 Inhibitors

Xinxian Deng^{a,b}, Jian Shen^{a,c}, Hui Zhu^d, Jia Xiao^a, Ran Sun^a, Fangzhou Xie^a, Celine Lam^a, Juntao Wang^a, Yixue Qiao^a, Mojdeh S. Tavallaie^a, Yang Hu^a, Yi Du^c, Jianqi Li^{b*}, Lei Fu^{a*} and Faqin Jiang^{a*}

a. School of Pharmacy, Shanghai Jiao Tong University, No. 800 Dongchuan Rd. Minhang District, Shanghai, 200240, China.

b. China State Institute of Pharmaceutical Industry, No. 285 Gebaini Rd. Pudong District Shanghai, 201203, China.

c. Viva Biotech Ltd. (Shanghai), No. 334 Aidisheng Rd., Pudong District Shanghai, 201203, China.

d. Department of Endocrinology, Shanghai Ninth People's Hospital, Shanghai Jiao Tong University School of Medicine, No. 369 Zhizaoju Road, Huangpu District, Shanghai, 200011, China

e. Xinhua hospital affiliated to Shanghai Jiao Tong University, School of Medicine, No. 1665 Kongjiang Rd., Yangpu District, Shanghai, 200092, China.

Abstract

The initial focus on characterizing novel pyrazolo[1,5-a]pyrimidin-7(4H)-one derivatives as DPP-4 inhibitors, led to a potent and selective inhibitor compound **b2**. This ligand exhibits potent *in vitro* DPP-4 inhibitory activity (IC₅₀: 80 nM), whilst maintaining other key cellular parameters such as high selectivity, low cytotoxicity and good cell viability. Subsequent optimization of **b2** based on docking analysis and structure-based drug design knowledge resulted in **d1**. Compound **d1** has nearly 2-fold increase of inhibitory activity (IC₅₀: 49 nM) and over 1000-fold selectivity against DPP-8 and DPP-9. Further *in vivo* IPGTT assays showed that compound **b2** effectively reduce glucose excursion by 34% at the dose of 10 mg/kg in diabetic mice. Herein we report the optimization and design of a potent and highly selective series of pyrazolo[1,5-a]pyrimidin-7(4H)-one DPP-4 inhibitors.

Key words

DPP-4 inhibitor; pyrazolo[1,5-a]pyrimidin-7(4H)-one derivatives; structure-based drug design; molecular docking; anti-diabetic.

*Corresponding authors. Tel./fax: +86 21 3420 4787 (Faqin Jiang.), +86 21 3420 4791 (Lei Fu.). E-mail addresses: lijianqb@126.com (Jianqi Li), [jq2008@sjtu.edu.cn](mailto:jfq2008@sjtu.edu.cn) (Faqin Jiang), leifu@sjtu.edu.cn (Lei Fu)

1. Introduction

Type 2 diabetes is one of the greatest impending global health concerns. To date 415 million people live with diabetes worldwide, and an estimated 193 million people have undiagnosed diabetes. Type 2 diabetes accounts for more than 90% of diabetes patients¹. Progressing efforts regarding risk factors for type 2 diabetes and some prevention programs have been proved to be resultful. But the incidence and widespread occurrence of the disease continues to rise globally and more than two-fold increase is expected over next 20 years. Among all discovered paths, the incretin pathway is emerging as a promising target for diabetes treatment². It facilitates a communication channel between the intestine and the endocrine pancreas and accounts for 50-70% of the total β cell derived insulin secretion in response to oral glucose ingestion². In fact, incretin-receptor activation is mainly occurred by glucagon like peptide-1 (GLP-1), one of the key hormones of this mechanism. GLP-1 stimulates the secretion of insulin after oral glucose absorption and as a result normalizes the blood glucose level³. On the other side, incretin is inactivated by the enzyme dipeptidyl peptidase (DPP-4) through catalyzing the hydrolyzation of GLP-1⁴. Therefore, therapeutic agents based on potentiation of incretin action provide new physiologically based approaches for the treatment of type 2 diabetes. For instance, the development of degradation-resistant GLP-1-receptor agonists or DPP-4 inhibitors would lead to increase plasma concentration of active GLP-1⁵. On recent advances in drug discovery, a variety of DPP-4 inhibitors with diverse structural features has been created as anti-diabetic drugs.

Unfortunately, the currently available DPP-4 inhibitors, as shown in Figure 1, are inevitably associated with several side effects such as nasopharyngitis, headache, nausea, hypersensitivity, skin reactions and pancreatitis. These side effects are caused due to the off-target effect: the inhibition of other DPP subtypes such as DPP-8 and DPP-9. To avoid those side effects, it's necessary to design advanced inhibitors with high activity for DPP-4 and great selectivity against other DPP subtypes as well.

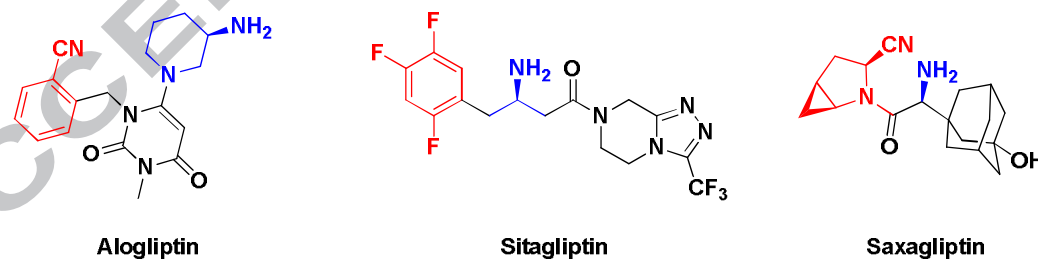


Figure 1. Key features of DPP-4 inhibitors.

Pyrazolo[1,5-a]pyrimidin derivatives are widely used in pharmaceutical industries⁶⁻⁸ and academic researches⁹⁻¹³ as lead compounds for the discovery of potential medical agents. However, they were never utilized as anti-diabetic candidates. The current study outlined the new approach towards creating a new series of DPP-4 inhibitors, with a focus on rational drug design and

structural optimization to pursue high *in vitro* activity, high selectivity and low cytotoxicity. To earn these benefits, we executed two strategies to generate new inhibitors as outlined in Figure 2. Firstly, we aimed to generate new class ligands by applying a novel core structure. By analyzing the structural components of the DPP-4 inhibitors, we found that the two key building blocks should be standing adjacent to each other with a distance of 1-2 atoms^{14, 15}. It suggests that the positions of the substitutions are important for activity. The skeleton of pyrazolo[1,5-a]pyrimidin-7(4H)-one perfectly meets the demand of such structural requirement, where substitutions can be attached to multiple contiguous positions. The π - π stacking between the core structure and Y547 would hopefully stabilize the overall conformation¹⁶. We then constructed 4, 5-substituted pyrazolo[1,5-a]pyrimidin-7(4H)-one analogs and discovered a novel series of DPP-4 inhibitors. Secondly, we study the nature of key building blocks. A hydrophobic or aromatic ring is needed to occupy the S1 pocket of DPP-4¹⁷⁻²⁰. The salt bridge between the ligand and E205/E206 residues plays a significant role for the generation of inhibition activity^{16, 21}. Based on such findings, we designed compounds with a substituted benzyl group on 4' position for the S1 occupation; and a cyclic amine group on 5' position for salt bridge networking. This approach could yield a unique series of DPP-4 inhibitors.

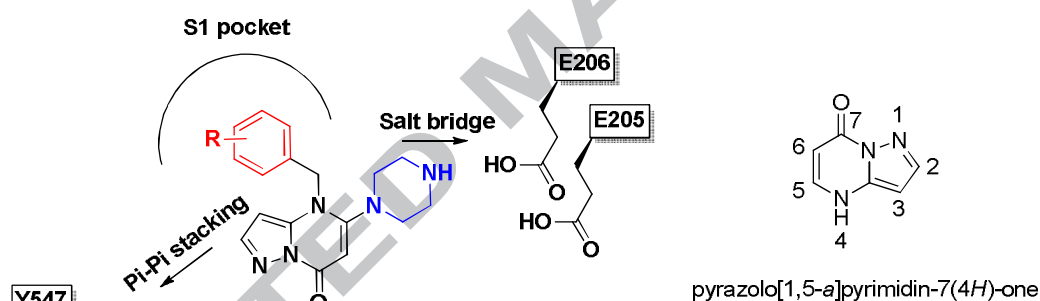


Figure 2. Design of novel DPP-4 inhibitors.

We herein report the design, synthesis and evaluation of biological activity of these newly designed compounds. We also highlight the key interactions between functional groups of synthesized compounds and DPP-4 active site residues for rational drug design.

2. Results and discussion

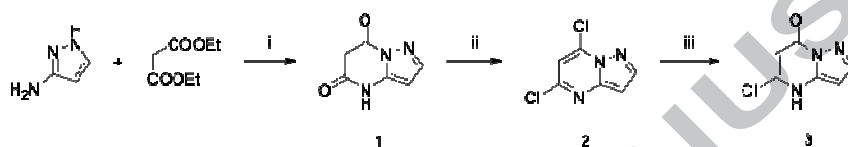
2.1 Chemistry

The synthesis of the target compounds is depicted in the following schemes. First of all, intermediate **3** (**Scheme 1**) was synthesized from two key intermediates. Intermediate **1** was obtained by the condensation and cyclization of 1H-pyrazol-5-amine and diethyl malonate. Chlorination of **1** with POCl₃ with N, N-dimethyl-aniline as the base, yielded the key product intermediate **2**. Compound **3** was produced via the hydrolyzation of **2** in 1 N NaOH aqueous

solution.

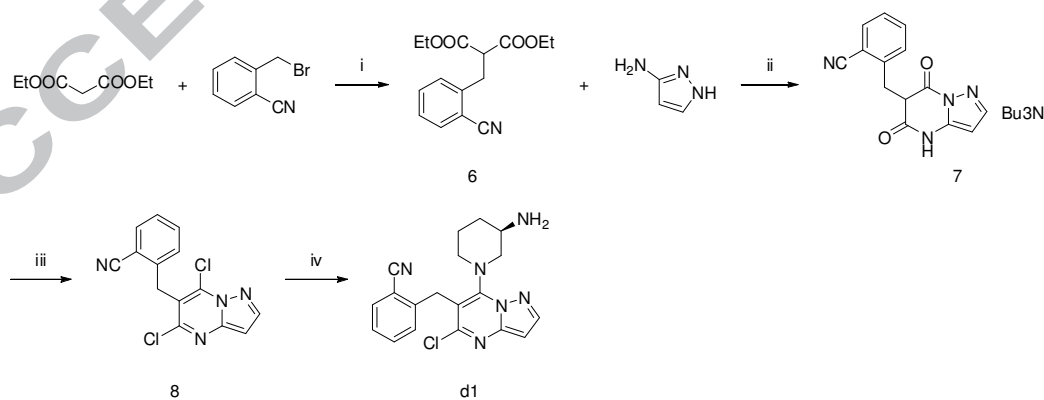
Starting from intermediate **3**, the syntheses of **b** series ligands were carried out following a synthetic route depicted below (**Scheme 2**). Intermediate **4** was synthesized by reacting **3** with corresponding benzyl halides under basic conditions, where Cs_2CO_3 or K_2CO_3 or DIPEA was used. The final compounds were converted from intermediate **4** where 2' Cl was substituted with two different amines followed by deprotection.

Compound **6** was made by the combination of 2-(bromomethyl)benzonitrile and diethyl malonate in EtOH using EtONa as the base (**Scheme 3**). A cyclization reaction was carried out to yield compound **7** which was chloridized by POCl_3 to form compound **8**. Compound **d1** was obtained by a substitution reaction on compound **8** with (R)-tert-butyl piperidin-3-yl carbamate at the final step.



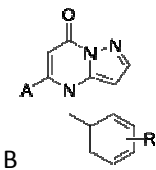
Scheme 1: i. EtONa EtOH, reflux; ii. POCl_3 , N,N-dimethyl-aniline, 100 °C; iii 1 N NaOH, 90 °C.

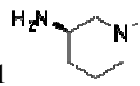
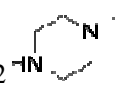
Scheme 2: i. Cs_2CO_3 or K_2CO_3 or DIPEA, DMF, 90 °C; ii. DIPEA, DMF, 90 °C; iii. TFA, DCM.



Scheme 3. i. EtONa, EtOH, r.t.; ii. Bu_3N , 180 °C; iii. POCl_3 , 110 °C; iv. (R)-tert-butyl piperidin-3-yl carbamate, TEA, THF, 60 °C; TFA, DCM.

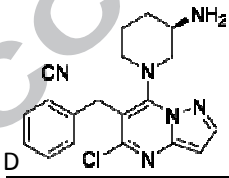
2.2 Biological evaluation and preliminary SAR analysis

Table 1. DPP-4 IC₅₀ values of b series compounds.


Structure features: A1  A2 

No.	Structure		DPP-4 IC ₅₀ (μM)
	A	R	
b1	A1	2-CN	1.3±0.45
b2	A2	2-CN	0.08±0.005
b3	A1	H	46.5±5.5
b4	A2	H	2.5±0.4
b5	A1	4-Me	2.0±0.4
b6	A2	4-Me	0.4±0.1
b7	A1	4-NO ₂	11.5±4.5
b8	A2	4-NO ₂	17.2±2.1
b9	A1	4-COOEt	10.4±0.9
b10	A1	4-COOH	59.9±4.4
b11	A1	2-F	21.5±1.3
b12	A2	2-NO ₂	1.2±0.6
Alogliptin			0.004±0.001

Values are means of three experiments. Data are represented as mean ± SD (*n* = 3)

Table 2. IC₅₀ values of d series compounds


No.	DPP-4 IC ₅₀ (μM)
d1	0.049±0.004

Values are means of three experiments. Data are represented as mean ± SD (*n* = 3)

The substituted benzyl group is supposed to stretch into the S1 pocket. We tried different functional groups in order to verify the impact brought by the substitutions on the benzyl ring. We found that placing a cyano group at *ortho* position could create the best inhibitory activity against

DPP-4 (**Table 1, b1** and **b2**). Cyano group in the S1 pocket has a typical effect improving the DPP-4 inhibitory activity in many successful DPP-4 inhibitors, such as alogliptin and vildagliptin. The same effect can also be obtained in our ligands. We explored the binding conformation of our ligands in the DPP-4 active site by molecular docking. In our docking model, the cyano group forms a H-bond with residue R125. This H-bond can be observed in the crystal structure 2NOC as well. We consider it as the reason why the cyano group can bring a typical effect to the DPP-4 ligands.

(R)-piperidin-3-amine is one of the structural features in a variety of DPP-4 inhibitors²¹⁻²⁵. Therefore we introduced the (R)-piperidin-3-amine to our compounds as a key component to generate the DPP-4 inhibitory activity. However, (R)-piperidin-3-amine was not the only choice at the same position²⁶⁻²⁸. For further evaluation of the amine group, piperazine was used as the substitution. Surprisingly, such a transformation brought significant activity improvement to the ligand. Among all of our synthetic compounds, those with the piperazine substitution have better DPP-4 IC₅₀ value than their counterparts with (R)-piperidin-3-amine substitution (**b2** vs **b1**, **b4** vs **b3**, **b6** vs **b5** and **b8** vs **b7**). A maximum of 18 times (**b4** vs **b3**) improvement was obtained with explained optimization. The most potent compound in **b** series is **b2**, which has DPP-4 IC₅₀ of 80 nM.

We performed molecule docking to study the binding of **b1** and **b2** in the protein in order to explain the activity differences. As is depicted in Figure 4A and 4B, compound **b1** and **b2** lie in the binding site where S1 pocket is occupied by the substituted benzyl ring. The amine of the two ligands forms H-bond interactions with E205 and E206. The one difference between the two ligands' binding is the number of the H-bonds. Compound **b1** forms an H-bond with E205 3.0 Å away. On the other hand, **b2** forms two H-bonds between the two amines and the two important acidic amino acids E205 and E206. The distances are 3.4 Å and 3.5 Å, respectively. The two molecules also forms H-bond between the -CN group and R125. Superimposition of the **b1** and the ligand in the crystal structure (PBD code: 2NOC) shows that they have similar interactions with the enzyme. What distinguishes them is the position and spatial configuration of the core structure. The pyrazolo[1,5-a]pyrimidin-7(4H)-one core of our compounds tends to stretch towards the enzyme while the ligand (IC₅₀ =13 nM) in co-crystal structure goes to another direction with larger space. We reasonably assumed that the reversal of the direction of the core structure may gain us a better inhibitory activity.

To generate a core-redirected ligand, we designed to switch the two substitutions' position. We put the benzonitrile group to 6' position and amine group to 7' position. Then we could obtain a ligand with a core reversal. Under the circumstances we created and synthesized compound **d1** to test the hypothesis (Table 2). The substitutions' positions swap could change the binding conformation of the core. Indeed, **d1** showed an improved inhibition activity against DPP-4 with IC₅₀ of 49 nM which is nearly 2 times better than **b2** and over 22 times stronger than **b1**. In DPP4-**d1** docking model (Figure 4D), we found a redirection of the core structure in the binding pocket. The cyano

substituted benzyn ring of **d1** occupied the S1 pocket. The salt bridge network between the (R)-piperidin-3-amine and E205 and E206 can also be observed. The R125 residue, however, forms a cation- π interaction with the core structure to further stabilize the conformation. These unique binding conformation along with the redirection of the core of **d1** boosts its inhibition activity.

We chose those with IC_{50} value less than 5 μM to perform the selectivity assay against DPP-8 and DPP-9 (Table 3). Results show that they all have good selectivity against the DPP-4 homologues proteins. Compound **b2** and **d1** have selectivity over DPP-8 and DPP-9 about 1000 times.

Table 3. DPP-8 and DPP-9 inhibitory activities of the selected compounds.

No.	DPP-8 IC_{50} (μM)	DPP-8/DPP-4	DPP-9 IC_{50} (μM)	DPP-9/DPP-4
b1	>100	>100	>100	>100
b2	>100	>1000	>100	>1000
b4	>100	>40	>100	>40
b5	>100	>50	>100	>50
b6	>100	>200	>100	>200
b12	>100	>100	>100	>100
d1	>100	>1000	>100	>1000

Values are means of three experiments.

2.3 Cytotoxicity assay

We performed MTT assay to determine the effects of compounds **b2** and **d1** on cell growth rate and viability. As is shown (Figure 3), **b2** and **d1** present a dose dependent manner in cell viability. As is demonstrated in the chart, cell viability of **b2** at 100 μM is more than 60%. In comparison **d1** shows a dramatic decrease viable cells at the same dose. The low cytotoxicity of **d1** at the dose of 20 μM or less is confident. Overall compound **b2** clearly shows a significant low cytotoxicity while compared to **d1**.

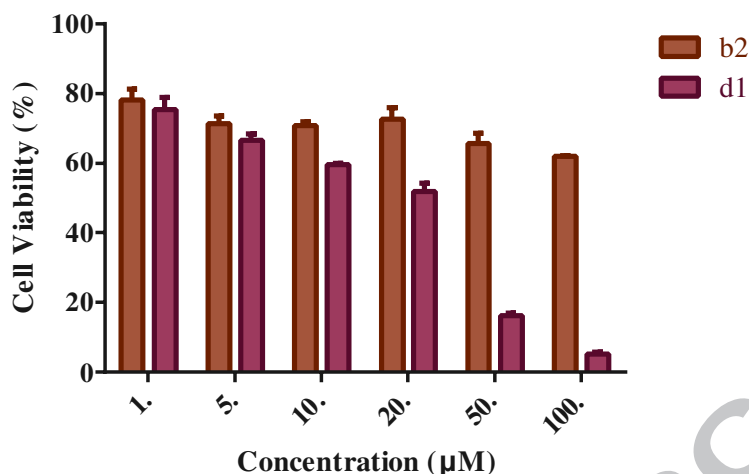
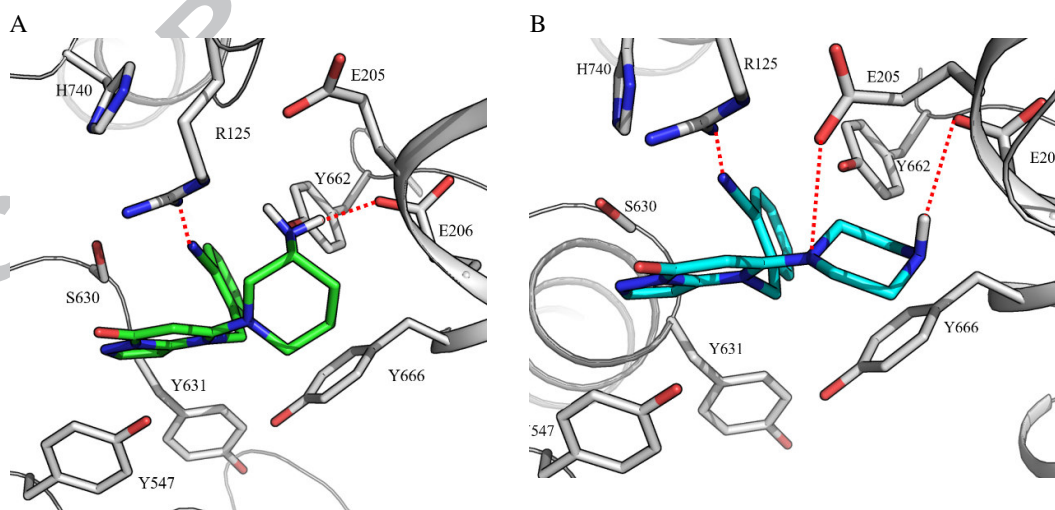


Figure 3. Inhibitory effect of compound **b2** and **d1** on the viability of HepG2 cells after 48 hrs is evaluated by MTT test. Each value was presented as mean \pm SD, $n=3$.

2.4 Molecular docking study

Interactions between ligands and DPP-4 (PDB code: 2ONC) are explained by molecular modeling using GOLD Suite v5.0.1. (CCDC, Cambridge, U.K., 2010). Before docking was run, parameters were specifically addressed. The binding site was defined to include all residues within a 15.0 Å radius of the E205 C γ carbon atom. An H-bond was restricted between the amine of the ligand ((R)-piperidin-3-amine or piperazine) and E205 of the enzyme. After the docking runs were completed, 20 conformations were produced for each ligand and GoldScore was used as scoring function. Other parameters were set as standard default. High-scoring complexes were inspected visually for selecting the most reasonable solution.



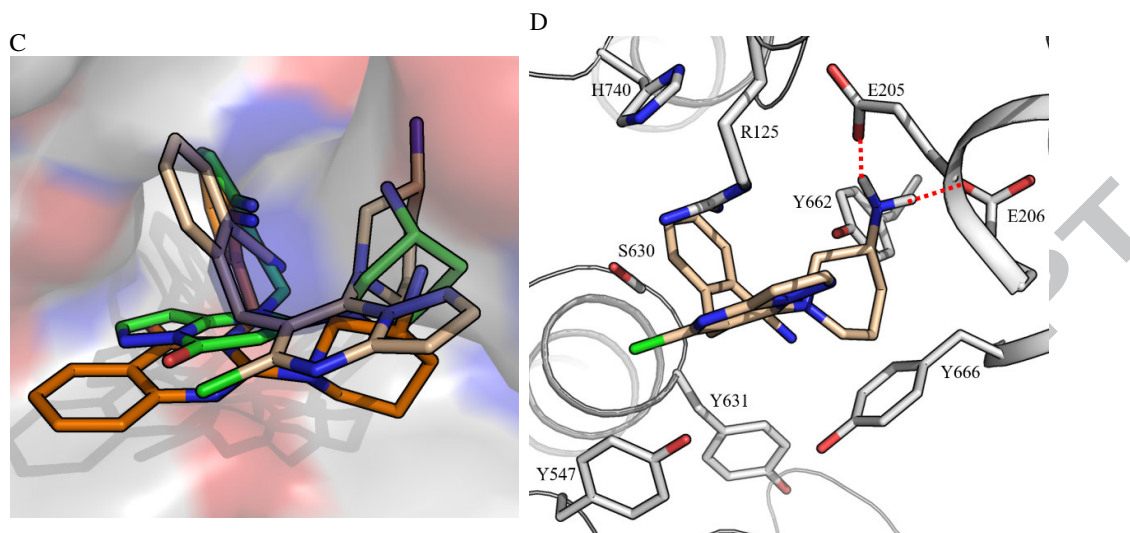


Figure 4. Docking of **b1** and **b2** to the DPP-4 model; A. compound **b1** is colored in green, the protein and the residues are colored in white; B. **b2** is colored in cyan, the protein and the residues are colored in white; C. Superimpose of the docking results to the crystal structure 2NOC, the protein is depicted with surface, **b1** is colored in green, **d1** is colored in gold, ligand in the crystal is colored in orange; D. compound **d1** is colored in gold, the protein and the residues are colored in white.

2.5 IPGTT assay

The in vivo hypoglycemic effects of compounds **b2** was evaluated in an intraperitoneal injection glucose tolerance test (IPGTT) using diabetic male C57BL/6 mice. Single intraperitoneal injection (IP) administration of **b2** to male BALB/c mice 30 min prior to an IPGTT reduced plasma glucose excursion in a dose-dependent manner from 1 mg/kg to 10 mg/kg. The results are shown in Table 4 and Figure 5. Intraperitoneal injection of **b2** at a dose of 10 mg/kg significantly reduced plasma glucose levels in male BALB/c mice by 34%, which transcended the effect of metformin (20% reduction, Figure 5) at the same dose.

The dose-dependent effects of compound **b2** in the IPGTT are shown in Figure 5. The results indicate that compound **b2** produced a dose-dependent improvement of glucose tolerance in diabetic male BALB/c mice after injection and its minimum effective dose was 1 mg/kg (Figure 5B).

Therefore, the potent and selective DPP-4 inhibitor **b2** is expected to provide a potential therapeutic efficacy for the treatment of type 2 diabetes.

Table 4. IPGTT assays of compound **b2** in diabetic mice.

	Blood glucose (mM)					AUC
	0 h	0.5 h	1 h	1.5 h	2 h	
Control	15.6±2.4	33.6±2.3	25.0±1.2	23.9±2.9	23.9±0.7	51.2±3.9
b2						

1 mg/kg	12.1±0.3	27.3±1.2	21.9±2.0	18.1±1.9	14.1±2.3	38.7±3.4
5 mg/kg	13.2±0.2	21.9±1.2	20.8±2.0	17.8±1.9	14.8±2.3	37.3±3.1
10 mg/kg	11.6±0.2	20.2±0.4	18.6±1.2	15.6±1.6	14.3±3.5	33.7±2.5
Metformin						
10 mg/kg	12.9±2.4	23.4±2.5	21.3±1.5	19.4±4.6	21.4±5.7	40.7±6.3

Data are represented as mean ± SD ($n = 4$)

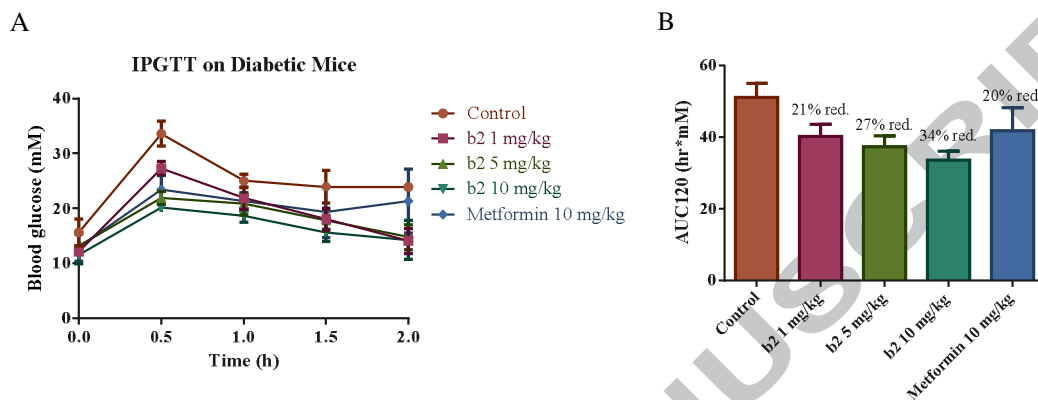


Figure 5. A. Effects of compound **b2** in various concentrations and 10 mg/kg metformin on glucose levels after an intraperitoneal injection glucose tolerance test in diabetic BALB/c male mice. Compound **b2** or saline (control) was administered 30 min prior to an injected dextrose challenge (2 g/kg). B. The glucose AUC was determined from 0-120 min. Percent reduction values for each treatment were generated from the AUC data normalized to the saline-challenged controls.

3. Conclusion

We have constructed a series of potent and greatly selective DPP-4 inhibitors with pyrazolo[1,5-*a*]pyrimidin-7(4H)-one core surrogates. The modification of the core led us to **b2** which has IC_{50} of 80 nM and > 1000 fold selectivity over DPP-8 and DPP-9. We utilized docking program to study the interactions between the ligand and the enzyme. We discovered that in our model the substituted benzyl ring occupies the S1 pocket, and the amine substitution forms H-bond interactions with the key residue E205 and E206. Through the comparison of our model to the co-crystal structure 2NOC, this hypothesis came up that the core structure might have an impact on the ligand activity. Therefore we designed and synthesized **d1** to redirect the core structure. As a result of this act the performance of the ligand improved immensely. Compound **d1** has DPP-4 IC_{50} of 49 nM and more than 1000 fold selectivity over DPP8 and DPP-9. Although **d1** has DPP-4 IC_{50} result greater than **b2**, yet **b2** is considerably less cytotoxic. Further *in vivo* IPGTT assay further indicated that compound **b2** exert positive impact on the diabetic male mice. To sum up, we have identified a series of new derivatives as well potent DPP-4 inhibitors. Compounds **b2** and **d1** possess good DPP-4 inhibitory activity, remarkable selectivity over other DPP subtypes such as DPP-8 and DPP-9, low cytotoxicity, and excellent *in vitro* and *in vivo* efficacy. It produced a

potential therapeutic efficacy for the treatment of type 2 diabetes.

4. Experimental Section

Chemistry

General Chemistry Procedure: All references to EA are diethyl ether; brine refers to a saturated aqueous solution of NaCl. Unless otherwise indicated, all temperatures are expressed in °C (degrees Centigrade). All reactions conducted under an inert atmosphere at room temperature unless otherwise noted. ¹H NMR spectra were recorded on an Agilent 400 MHz NMR. ¹³C NMR spectra were recorded on an Agilent 100 MHz NMR. Chemical shifts are expressed in parts per million (ppm). Coupling constants are in units of Hertz (Hz). Splitting patterns describe apparent multiplicities and are designated as s (singlet), d (doublet), t (triplet), q (quartet), m (multiplet) and br (broad). High-resolution mass spectra (HRMS) and compound purity data were acquired on an Agilent 6200 TOF LC/MS system, UV detector (220 and 254 nm).

4.1. General procedure A:

To a solution of 5-chloropyrazolo[1,5-a]pyrimidin-7(4H)-one (1 eq) in DMF was added 2 eq. of Cs₂CO₃ or K₂CO₃ or DIPEA and the corresponding (bromomethyl)benzene analog. The reaction was heated to 90 °C overnight. After the completion of the reaction, EA and water were added, the organic layer was washed with water 3 times. Collect the organic layer, remove the solvent to obtain the crude product. The crude product was purified by F.C.C. to obtain the corresponding product.

4.1.1. 4-benzyl-5-chloropyrazolo[1,5-a]pyrimidin-7(4H)-one (**4a**): This compound is synthesized according to general procedure A (yield: 68.56%); ¹H NMR (400 MHz, CHLOROFORM-d) δ 7.66 (d, *J* = 1.00 Hz, 1H), 7.33 - 7.48 (m, 5H), 6.36 (d, *J* = 3.52 Hz, 1H), 6.07 (s, 1H), 5.97 (s, 2H); HRMS (ESI): calcd for C₁₃H₁₁ClN₃O [M + H]⁺ 260.0591; found 260.0587.

4.1.2. 2-((5-chloro-7-oxopyrazolo[1,5-a]pyrimidin-4(7H)-yl)methyl)benzotrile (**4b**): This compound is synthesized according to general procedure A (yield: 59.56%); ¹H NMR (400 MHz, CHLOROFORM-d) δ 8.03 (d, *J* = 3.52 Hz, 1H), 7.70 (d, *J* = 7.83 Hz, 1H), 7.54 - 7.65 (m, 2H), 7.37 - 7.51 (m, 1H), 6.42 (d, *J* = 3.52 Hz, 1H), 6.22 (s, 2H), 6.15 (s, 1H); HRMS (ESI): calcd for C₁₄H₁₀ClN₄O [M + H]⁺ 285.0543; found 285.0567.

4.1.3. 4-((5-chloro-7-oxopyrazolo[1,5-a]pyrimidin-4(7H)-yl)methyl)benzotrile (**4c**): This compound is synthesized according to general procedure A (yield: 59.56%); ¹H NMR (400 MHz, CHLOROFORM-d) δ 7.75 (d, *J* = 3.13 Hz, 1H), 7.59 (d, *J* = 7.83 Hz, 2H), 7.21 - 7.26 (m, 2H), 6.40 (d, *J* = 3.13 Hz, 1H), 6.02 (s, 1H), 5.98 (s, 2H); HRMS (ESI): calcd for C₁₄H₁₀ClN₄O [M + H]⁺ 285.0543; found 285.0567.

4.1.4. ethyl 4-((5-chloro-7-oxopyrazolo[1,5-a]pyrimidin-4(7H)-yl)methyl)benzoate (**4d**): This compound is synthesized according to general procedure A (yield: 51.11%); ^1H NMR (400 MHz, CHLOROFORM-*d*) δ 7.53 (d, $J = 7.83$ Hz, 2H), 7.30 - 7.40 (m, 2H), 7.16 (s, 1H), 7.00 (d, $J = 1.00$ Hz, 1H), 6.21 (s, 1H), 5.42 (s, 2H), 4.38 (q, $J = 7.00$ Hz, 2H), 1.40 (t, $J = 1.00$ Hz, 3H); HRMS (ESI): calcd for $\text{C}_{16}\text{H}_{15}\text{ClN}_3\text{O}_3$ $[\text{M} + \text{H}]^+$ 332.0802; found 332.0811.

4.1.5. 5-chloro-4-(2-fluorobenzyl)pyrazolo[1,5-a]pyrimidin-7(4H)-one (**4e**): This compound is synthesized according to general procedure A (yield: 61.07%); ^1H NMR (400 MHz, CHLOROFORM-*d*) δ 7.78 (br. d, $J = 1.00$ Hz, 1H), 7.41 - 7.56 (m, 1H), 7.33 (d, $J = 6.65$ Hz, 1H), 6.97 - 7.19 (m, 2H), 6.35 (d, $J = 3.13$ Hz, 1H), 6.10 (s, 1H), 6.05 (s, 2H); HRMS (ESI): calcd for $\text{C}_{13}\text{H}_{10}\text{ClFN}_3\text{O}$ $[\text{M} + \text{H}]^+$ 278.0496; found 278.0482.

4.1.6. 5-chloro-4-(4-nitrobenzyl)pyrazolo[1,5-a]pyrimidin-7(4H)-one (**4f**): This compound is synthesized according to general procedure A (yield: 45.91%); ^1H NMR (400 MHz, CHLOROFORM-*d*) δ 8.20 (d, $J = 8.61$ Hz, 2H), 7.79 (d, $J = 3.52$ Hz, 1H), 7.36 (d, $J = 8.61$ Hz, 2H), 6.47 (d, $J = 3.13$ Hz, 1H), 6.08 (br. s., 1H), 6.07 (s, 2H); HRMS (ESI): calcd for $\text{C}_{13}\text{H}_{10}\text{ClN}_4\text{O}_3$ $[\text{M} + \text{H}]^+$ 305.0441; found 305.0451.

4.1.7. 5-chloro-4-(4-methylbenzyl)pyrazolo[1,5-a]pyrimidin-7(4H)-one (**4g**): ^1H NMR (400 MHz, CHLOROFORM-*d*) δ 7.65 (d, $J = 3.13$ Hz, 1H), 7.10 - 7.18 (m, 4H), 6.35 (d, $J = 3.13$ Hz, 1H), 6.08 (s, 1H), 5.92 (s, 2H), 2.33 (s, 3H); HRMS (ESI): calcd for $\text{C}_{14}\text{H}_{13}\text{ClN}_3\text{O}$ $[\text{M} + \text{H}]^+$ 274.0747; found 274.0755.

4.1.8. 5-chloro-4-(2-nitrobenzyl)pyrazolo[1,5-a]pyrimidin-7(4H)-one (**4h**): This compound is synthesized according to general procedure A (yield: 66.28%); ^1H NMR (400 MHz, CHLOROFORM-*d*) δ 8.13 (d, $J = 7.83$ Hz, 1H), 7.81 (d, $J = 3.52$ Hz, 2H), 7.59 (t, $J = 7.43$ Hz, 1H), 7.52 (t, $J = 7.83$ Hz, 1H), 7.00 (d, $J = 7.43$ Hz, 1H), 6.45 (s, 2H), 6.04 (s, 1H); HRMS (ESI): calcd for $\text{C}_{13}\text{H}_{10}\text{ClN}_4\text{O}_3$ $[\text{M} + \text{H}]^+$ 305.0441; found 305.0433.

4.2. General procedure B.

To a solution of 4-benzyl-5-chloropyrazolo[1,5-a]pyrimidin-7(4H)-one analogs, piperazine or (R)-tert-butyl piperidin-3-ylcarbamate and DIPEA in DMF was heated to 90 °C overnight. After the completion of the reaction, EA was added to the reaction mixture and washed with water $\times 3$. The organic layer was collected. Removed the solvent to obtain the crude product. The crude was purified by F.C.C. to obtain the desired product.

4.2.1. (R)-tert-butyl (1-(4-(2-cyanobenzyl)-7-oxo-4,7-dihydropyrazolo[1,5-a]pyrimidin-5-

yl)piperidin-3-yl)carbamate (**5a**): This compound is synthesized according to general procedure B (yield: 31.74%); $^1\text{H NMR}$ (400 MHz, CHLOROFORM-*d*) δ 8.03 (d, $J = 3.52$ Hz, 1H), 7.70 (d, $J = 7.83$ Hz, 1H), 7.54 - 7.65 (m, 2H), 7.37 - 7.51 (m, 1H), 6.42 (d, $J = 3.52$ Hz, 1H), 6.22 (s, 2H), 6.15 (s, 1H), 3.64 (d, $J = 10.62$ Hz, 2H), 3.25 (d, $J = 12.51$ Hz, 2H), 1.91 - 2.15 (m, 2H), 1.66 - 1.79 (m, 2H), 1.50 - 1.61 (m, 1H), 1.45 (br. s., 9H); HRMS (ESI): calcd for $\text{C}_{24}\text{H}_{29}\text{N}_6\text{O}_3$ [$\text{M} + \text{H}$] $^+$ 449.2301; found 449.2364.

4.2.2. (R)-tert-butyl (1-(4-benzyl-7-oxo-4,7-dihydropyrazolo[1,5-*a*]pyrimidin-5-yl)piperidin-3-yl)carbamate (**5b**): This compound is synthesized according to general procedure B (yield: 30.88%); $^1\text{H NMR}$ (400 MHz, CHLOROFORM-*d*) δ 8.00 (s, 1H), 7.50 (d, $J = 3.13$ Hz, 1H), 7.28 - 7.39 (m, 2H), 7.17 - 7.27 (m, 2H), 6.07 (br. d, $J = 1.00$ Hz, 1H), 5.80 (s, 2H), 5.33 (s, 1H), 4.54 - 4.78 (m, 2H), 3.49 - 3.93 (m, 2H), 2.96 (s, 2H), 1.81 - 2.14 (m, 2H), 1.70 (d, $J = 10.96$ Hz, 1H), 1.45 (br. s., 9H); HRMS (ESI): calcd for $\text{C}_{23}\text{H}_{30}\text{N}_5\text{O}_3$ [$\text{M} + \text{H}$] $^+$ 424.2349; found 424.2361.

4.2.3. (R)-ethyl 4-((5-(3-((tert-butoxycarbonyl)amino)piperidin-1-yl)-7-oxopyrazolo[1,5-*a*]pyrimidin-4(7H)-yl)methyl)benzoate (**5c**): This compound is synthesized according to general procedure B (yield: 55.79%); $^1\text{H NMR}$ (400 MHz, CHLOROFORM-*d*) δ 7.53 (d, $J = 7.83$ Hz, 2H), 7.30 - 7.40 (m, 2H), 7.16 (s, 1H), 7.00 (d, $J = 1.00$ Hz, 1H), 6.21 (s, 1H), 5.42 (s, 2H), 4.55 (br. s., 1H), 4.33 - 4.47 (m, 2H), 3.02 - 3.73 (m, 6H), 1.97 (br. s., 1H), 1.59 (s, 9H), 1.40 (t, $J = 1.00$ Hz, 3H), 1.26 (br. s., 1H); HRMS (ESI): calcd for $\text{C}_{26}\text{H}_{34}\text{N}_5\text{O}_5$ [$\text{M} + \text{H}$] $^+$ 496.2560; found 496.2483.

4.2.4. (R)-tert-butyl (1-(4-(2-fluorobenzyl)-7-oxo-4,7-dihydropyrazolo[1,5-*a*]pyrimidin-5-yl)piperidin-3-yl)carbamate (**5d**): This compound is synthesized according to general procedure B (yield: 55.79%); $^1\text{H NMR}$ (400 MHz, CHLOROFORM-*d*) δ 7.78 (br. d, $J = 1.00$ Hz, 1H), 7.41 - 7.56 (m, 1H), 7.33 (d, $J = 6.65$ Hz, 1H), 6.97 - 7.19 (m, 2H), 6.35 (d, $J = 3.13$ Hz, 1H), 6.10 (s, 1H), 6.05 (s, 2H), 4.09 - 4.27 (m, 1H), 3.92 (d, $J = 6.10$ Hz, 2H), 3.58 (br. s., 1H), 3.25 - 3.50 (m, 1H), 2.28 (br. s., 2H), 2.14 (br. s., 1H), 1.44 (m, 9H), 1.22 - 1.31 (m, 1H); HRMS (ESI): calcd for $\text{C}_{23}\text{H}_{29}\text{FN}_5\text{O}_3$ [$\text{M} + \text{H}$] $^+$ 442.2254; found 442.2311.

4.2.5. (R)-tert-butyl (1-(4-(4-methylbenzyl)-7-oxo-4,7-dihydropyrazolo[1,5-*a*]pyrimidin-5-yl)piperidin-3-yl)carbamate (**5e**): This compound is synthesized according to general procedure B (yield: 14.38%); $^1\text{H NMR}$ (400 MHz, CHLOROFORM-*d*) δ 7.47 (d, $J = 2.74$ Hz, 1H), 7.05 - 7.21 (m, 4H), 6.06 (d, $J = 4.30$ Hz, 1H), 5.75 (s, 2H), 5.33 (s, 1H), 4.58 (br. s., 1H), 3.64 (d, $J = 10.96$ Hz, 2H), 3.18 - 3.47 (m, 2H), 2.31 (s, 3H), 1.96 (br. s., 1H), 1.64 - 1.92 (m, 2H), 1.45 (br. s., 9H), 1.22 - 1.31 (m, 1H); HRMS (ESI): calcd for $\text{C}_{24}\text{H}_{32}\text{N}_5\text{O}_3$ [$\text{M} + \text{H}$] $^+$ 438.2505; found 438.2606

4.2.6. (R)-tert-butyl (1-(4-(4-nitrobenzyl)-7-oxo-4,7-dihydropyrazolo[1,5-*a*]pyrimidin-5-

yl)piperidin-3-yl)carbamate (**5f**): This compound is synthesized according to general procedure B (yield: 54.38%); $^1\text{H NMR}$ (400 MHz, CHLOROFORM-*d*) δ 8.20 (d, $J = 8.61$ Hz, 2H), 7.79 (d, $J = 3.52$ Hz, 1H), 7.36 (d, $J = 8.61$ Hz, 2H), 6.47 (d, $J = 3.13$ Hz, 1H), 6.08 (br. s., 1H), 6.07 (s, 2H), 3.81 (br. s., 1H), 3.65 (d, $J = 10.17$ Hz, 2H), 3.48 (br. s., 2H), 3.25 (br. s., 2H), 1.91 - 2.17 (m, 2H), 1.41 - 1.46 (m, 9H); HRMS (ESI): calcd for $\text{C}_{23}\text{H}_{29}\text{N}_6\text{O}_5$ $[\text{M} + \text{H}]^+$ 469.2199; found 469.2239.

4.3. General procedure C.

To a solution of compound 8 in DCM was treated with TFA in a ratio of 1/10 v/v. The reaction was monitored with TLC. After the completion of the reaction, the solvent was removed by vacuum and the crude was purified by F.C.C. to obtain the desired product.

4.3.1. (R)-2-((5-(3-aminopiperidin-1-yl)-7-oxopyrazolo[1,5-*a*]pyrimidin-4(7H)-yl)methyl)benzotrile (**b1**): This compound is synthesized according to general procedure C (yield: 61.15%); m.p. = 138-140 °C; $^1\text{H NMR}$ (400 MHz, CHLOROFORM-*d*) δ 8.03 (d, $J = 3.52$ Hz, 1H), 7.70 (d, $J = 7.83$ Hz, 1H), 7.54 - 7.65 (m, 2H), 7.37 - 7.51 (m, 1H), 6.42 (d, $J = 3.52$ Hz, 1H), 6.22 (s, 2H), 6.15 (s, 1H), 3.64 (d, $J = 10.62$ Hz, 2H), 3.25 (d, $J = 12.51$ Hz, 2H), 1.91 - 2.15 (m, 2H), 1.66 - 1.79 (m, 2H), 1.50 - 1.61 (m, 1H); $^{13}\text{C NMR}$ (CHLOROFORM-*d*) δ : 161.7, 160.5, 157.8, 140.9, 139.8, 137.6, 133.1, 130.4, 129.1, 117.6, 111.1, 98.9, 80.9, 52.9, 45.4, 45.0, 44.1, 39.7, 29.6; HRMS (ESI): calcd for $\text{C}_{19}\text{H}_{21}\text{N}_6\text{O}$ $[\text{M} + \text{H}]^+$ 349.1777; found 349.1792.

4.3.2. 2-((7-oxo-5-(piperazin-1-yl)pyrazolo[1,5-*a*]pyrimidin-4(7H)-yl)methyl)benzotrile (**b2**): This compound is synthesized according to general procedure B (yield: 5.88%); m.p. = 102-104 °C; $^1\text{H NMR}$ (400 MHz, CHLOROFORM-*d*) δ 8.12 (d, $J = 1.00$ Hz, 1H), 7.85 (br. s., 1H), 7.64 (d, $J = 6.65$ Hz, 2H), 7.55 (t, $J = 7.24$ Hz, 1H), 6.13 (br. s., 1H), 6.07 (s, 2H), 5.39 (d, $J = 1.00$ Hz, 1H), 3.57 - 3.66 (m, 4H), 3.41 - 3.51 (m, 4H); $^{13}\text{C NMR}$ (101 MHz, CHLOROFORM-*d*) δ 160.9, 158.8, 141.7, 139.8, 137.6, 133.4, 133.1, 130.4, 129.1, 117.4, 111.7, 98.9, 80.9, 52.9, 45.0, 44.1, 39.7, 28.3; HRMS (ESI): calcd for $\text{C}_{18}\text{H}_{19}\text{N}_6\text{O}$ $[\text{M} + \text{H}]^+$ 335.1620; found 335.1615.

4.3.3. (R)-5-(3-aminopiperidin-1-yl)-4-benzylpyrazolo[1,5-*a*]pyrimidin-7(4H)-one (**b3**): This compound is synthesized according to general procedure C (yield: 22.70%); m.p. = 110-112 °C; $^1\text{H NMR}$ (400 MHz, CHLOROFORM-*d*) δ 7.44 (d, $J = 3.52$ Hz, 1H), 7.27 - 7.33 (m, 2H), 7.14 - 7.24 (m, 3H), 6.01 (d, $J = 3.13$ Hz, 1H), 5.75 (s, 2H), 5.43 (s, 1H), 4.16 (d, $J = 12.52$ Hz, 1H), 3.91 (d, $J = 12.91$ Hz, 1H), 3.72 (q, $J = 6.78$ Hz, 1H), 3.29 - 3.41 (m, 1H), 3.12 - 3.29 (m, 2H), 2.08 (br. s., 1H), 1.69 - 1.83 (m, 2H); $^{13}\text{C NMR}$ (101 MHz, CHLOROFORM-*d*) δ 161.7, 159.0, 152.9, 139.4, 134.4, 128.8, 128.4, 128.0, 98.0, 80.4, 55.7, 48.8, 47.2, 44.6, 29.4, 22.7; HRMS (ESI): calcd for $\text{C}_{18}\text{H}_{22}\text{N}_5\text{O}$ $[\text{M} + \text{H}]^+$ 324.1824; found 324.1983.

4.3.4. 4-benzyl-5-(piperazin-1-yl)pyrazolo[1,5-a]pyrimidin-7(4H)-one (**b4**): This compound is synthesized according to general procedure B (yield: 31.59%); m.p. = 100-102 °C; ¹H NMR (400 MHz, CHLOROFORM-d) δ 8.12 (s, 1H), 7.53 (d, *J* = 3.13 Hz, 1H), 7.27 - 7.33 (m, 4H), 6.10 (d, *J* = 3.52 Hz, 1H), 5.84 (s, 2H), 5.31 (s, 1H), 3.60 (t, *J* = 1.00 Hz, 4H), 3.44 (t, *J* = 4.89 Hz, 4H); ¹³C NMR (101 MHz, CHLOROFORM-d) δ 160.8, 158.8, 153.2, 139.2, 134.2, 128.9, 128.6, 128.3, 98.2, 80.9, 55.8, 45.4, 45.1, 44.2, 39.8; HRMS (ESI): calcd for C₁₇H₂₀N₅O [M + H]⁺ 310.1668; found 310.1664.

4.3.5. (R)-5-(3-aminopiperidin-1-yl)-4-(4-methylbenzyl)pyrazolo[1,5-a]pyrimidin-7(4H)-one (**b5**): This compound is synthesized according to general procedure C (yield: 59.65%); m.p. = 132-134 °C; ¹H NMR (400 MHz, CHLOROFORM-d) δ 7.39 (br. d, *J* = 1.00 Hz, 1H), 6.99 - 7.18 (m, 4H), 5.99 (br. s., 1H), 5.62 - 5.79 (m, 2H), 5.50 (br. d, *J* = 1.00 Hz, 1H), 4.09 - 4.27 (m, 2H), 3.93 (d, *J* = 6.13 Hz, 1H), 3.58 (br. s., 1H), 3.25 - 3.50 (m, 1H), 3.13 (d, *J* = 6.65 Hz, 2H), 2.28 (br. s., 3H), 2.14 (br. s., 1H), 1.53 (br. s., 1H); ¹³C NMR (101 MHz, CHLOROFORM-d) δ 161.7, 152.9, 139.3, 138.4, 131.3, 129.6, 128.2, 97.9, 80.6, 77.3, 55.6, 47.2, 45.8, 44.5, 28.6, 22.6, 21.1; HRMS (ESI): calcd for C₁₉H₂₄N₅O [M + H]⁺ 338.1981; found 338.2091.

4.3.6. 4-(4-methylbenzyl)-5-(piperazin-1-yl)pyrazolo[1,5-a]pyrimidin-7(4H)-one (**b6**): This compound is synthesized according to general procedure B (yield: 19.47%); m.p. = 112-114 °C; ¹H NMR (400 MHz, CHLOROFORM-d) δ 7.49 (d, *J* = 3.13 Hz, 1H), 7.06 - 7.18 (m, 4H), 6.06 (d, *J* = 3.52 Hz, 1H), 5.76 (s, 2H), 5.29 (s, 1H), 3.51 - 3.66 (m, 2H), 3.32 - 3.42 (m, 2H), 2.87 (td, *J* = 4.94, 17.51 Hz, 4H), 2.30 (s, 3H); ¹³C NMR (101 MHz, CHLOROFORM-d) δ 160.1, 146.9, 138.4, 130.5, 128.8, 128.7, 127.7, 127.6, 97.5, 79.6, 54.8, 46.0, 45.0, 40.4, 28.9, 20.3; HRMS (ESI): calcd for C₁₈H₂₂N₅O [M + H]⁺ 324.1824; found 324.1844.

4.3.7. (R)-5-(3-aminopiperidin-1-yl)-4-(4-nitrobenzyl)pyrazolo[1,5-a]pyrimidin-7(4H)-one (**b7**): This compound is synthesized according to general procedure C (yield: 59.65%); m.p. = 124-126 °C; ¹H NMR (400 MHz, CHLOROFORM-d) δ 8.20 (d, *J* = 8.61 Hz, 2H), 7.79 (d, *J* = 3.52 Hz, 1H), 7.36 (d, *J* = 8.61 Hz, 2H), 6.47 (d, *J* = 3.13 Hz, 1H), 6.08 (br. s., 1H), 6.07 (s, 2H), 3.81 (br. s., 1H), 3.65 (d, *J* = 10.17 Hz, 2H), 3.48 (br. s., 2H), 3.25 (br. s., 2H), 1.91 - 2.17 (m, 2H); ¹³C NMR (CHLOROFORM-d) δ: 160.9, 160.8, 148.6, 141.7, 133.7, 131.1, 128.6, 128.1, 124.0, 123.6, 46.0, 45.3, 44.9, 40.5, 39.4, 30.0; HRMS (ESI): calcd for C₁₈H₂₁N₆O₃ [M + H]⁺ 369.1675; found 369.1692.

4.3.8. 4-(4-nitrobenzyl)-5-(piperazin-1-yl)pyrazolo[1,5-a]pyrimidin-7(4H)-one (**b8**): This compound is synthesized according to general procedure B (yield: 19.78%); m.p. = 114-116 °C; ¹H NMR (400 MHz, CHLOROFORM-d) δ 8.33 (d, *J* = 8.20 Hz, 1H), 8.17 (d, *J* = 8.40 Hz, 1H), 8.08 - 8.14 (m, 2H), 8.00 (d, *J* = 8.61 Hz, 1H), 7.93 (s, 1H), 7.60 (d, *J* = 8.22 Hz, 1H), 3.66 - 3.71

(m, 2H), 3.59 - 3.66 (m, 2H), 3.57 (s, 1H), 3.48 - 3.54 (m, 2H), 3.44 (s, 1H), 3.35 - 3.42 (m, 2H); ^{13}C NMR (101 MHz, CHLOROFORM-*d*) δ 160.9, 160.8, 148.6, 141.7, 133.7, 131.1, 128.6, 128.1, 124.0, 123.6, 46.0, 44.9, 40.5, 39.4, 29.6; HRMS (ESI): calcd for $\text{C}_{17}\text{H}_{19}\text{N}_6\text{O}_3$ $[\text{M} + \text{H}]^+$ 355.1519; found 355.1576.

4.3.9. (R)-ethyl 4-((5-(3-aminopiperidin-1-yl)-7-oxopyrazolo[1,5-*a*]pyrimidin-4(7H)-yl)methyl)benzoate (**b9**): This compound is synthesized according to general procedure C (yield: 22.72%); m.p. = 134-136 °C; ^1H NMR (400 MHz, DMSO-*d*₆) δ 7.83 - 8.01 (m, 4H), 7.56 (d, J = 7.83 Hz, 1H), 7.35 - 7.50 (m, 2H), 5.07 - 5.36 (m, 2H), 4.66 - 4.93 (m, 2H), 4.28 (t, J = 7.04 Hz, 2H), 4.10 (d, J = 4.70 Hz, 1H), 3.93 (s, 2H), 1.87 - 2.01 (m, 2H), 1.23 - 1.31 (m, 3H), 0.75 - 0.86 (m, 2H); ^{13}C NMR (101 MHz, CHLOROFORM-*d*) δ 166.1, 162.9, 132.6, 130.4, 130.1, 130.0, 128.9, 128.8, 127.8, 127.7, 126.6, 61.2, 57.0, 29.8, 29.7, 29.6, 29.4, 29.3, 14.2; HRMS (ESI): calcd for $\text{C}_{21}\text{H}_{26}\text{N}_5\text{O}_3$ $[\text{M} + \text{H}]^+$ 396.2036; found 396.2108.

4.3.10. (R)-4-((5-(3-aminopiperidin-1-yl)-7-oxopyrazolo[1,5-*a*]pyrimidin-4(7H)-yl)methyl)benzoic acid (**b10**): To a solution of **b9** in EtOH was added 2 eq. NaOH and heated to reflux overnight. After the completion of the reaction, EtOH was removed by vacuum. The crude product was acidified by AcOH and purified by F.C.C. (yield: 20.70%); m.p. = 136-138 °C; ^1H NMR (400 MHz, CHLOROFORM-*d*) δ 8.04 (br. d, J = 1.00 Hz, 1H), 7.70 (d, J = 7.43 Hz, 1H), 7.59 (br. s., 2H), 7.39 - 7.53 (m, 1H), 6.42 (br. d, J = 1.00 Hz, 1H), 6.22 (s, 2H), 6.14 (s, 1H), 2.36 (s, 2H), 2.25 (br. s., 2H), 2.03 (br. s., 4H), 0.80 - 0.93 (m, 1H); ^{13}C NMR (101 MHz, CHLOROFORM-*d*) δ 169.3, 163.1, 143.2, 131.4, 130.8, 131.0, 128.9, 128.8, 128.0, 127.7, 126.6, 92.2, 57.0, 53.5, 50.4, 38.5, 22.3; HRMS (ESI): calcd for $\text{C}_{19}\text{H}_{22}\text{N}_5\text{O}_3$ $[\text{M} + \text{H}]^+$ 368.1723; found 368.1822.

4.3.11. (R)-5-(3-aminopiperidin-1-yl)-4-(2-fluorobenzyl)pyrazolo[1,5-*a*]pyrimidin-7(4H)-one (**b11**): This compound is synthesized according to general procedure C (yield: 32.33%); m.p. = 138-140 °C; ^1H NMR (400 MHz, CHLOROFORM-*d*) δ 7.78 (br. d, J = 1.00 Hz, 1H), 7.41 - 7.56 (m, 1H), 7.33 (d, J = 6.65 Hz, 1H), 6.97 - 7.19 (m, 2H), 6.35 (d, J = 3.13 Hz, 1H), 6.10 (s, 1H), 6.05 (s, 2H), 4.09 - 4.27 (m, 1H), 3.94 (d, J = 6.10 Hz, 2H), 3.58 (br. s., 1H), 3.25 - 3.50 (m, 1H), 2.28 (br. s., 2H), 2.14 (br. s., 1H), 1.22 - 1.31 (m, 1H); ^{13}C NMR (101 MHz, CHLOROFORM-*d*) δ 161.5, 161.2, 139.2, 139.1, 133.9, 128.9, 127.2, 125.6, 120.2, 119.1, 117.2, 114.3, 34.9, 28.7, 28.3, 26.2, 21.7, 13.1 ; HRMS (ESI): calcd for $\text{C}_{18}\text{H}_{21}\text{FN}_5\text{O}$ $[\text{M} + \text{H}]^+$ 342.1730; found 342.2113.

4.3.12. 4-(2-nitrobenzyl)-5-(piperazin-1-yl)pyrazolo[1,5-*a*]pyrimidin-7(4H)-one (**b12**): This compound is synthesized according to general procedure C (yield: 32.33%); m.p. = 106-108 °C; ^1H NMR (400 MHz, CHLOROFORM-*d*) δ 8.13 (d, J = 7.83 Hz, 1H), 7.81 (d, J = 3.52 Hz, 1H), 7.59 (t, J = 7.43 Hz, 1H), 7.52 (t, J = 7.83 Hz, 2H), 7.00 (d, J = 7.43 Hz, 1H), 6.45 (s, 2H), 6.04 (s,

1H), 3.64 - 3.71 (m, 2H), 3.52 - 3.64 (m, 4H), 3.36 - 3.47 (m, 2H); ¹³C NMR (101 MHz, CHLOROFORM-d) δ 160.0, 140.8, 133.6, 132.6, 130.1, 129.3, 126.9, 124.0, 123.5, 123.0, 118.1, 115.3, 30.4, 29.2, 28.7, 21.7, 13.1; HRMS (ESI): calcd for C₁₇H₁₉N₆O₃ [M + H]⁺ 354.1440; found 354.1476.

4.4.1. Diethyl 2-(2-cyanobenzyl)malonate (**6**): To a solution of 1 g (6.24 mM) diethyl malonate and 1.22 g (6.24 mM) 2-(bromomethyl)benzonitrile in EtOH was added 0.85 g (12.5 mM) EtONa at ice bath. The reaction mixture was stirred at ambient temperature overnight and monitored by TLC. After the completion of the reaction, EtOH was removed by vacuum. Then EA and 1N HCl solution were added to the mixture. The organic layer was washed with water 3 times and concentrated under vacuum. The crude product was purified by F.C.C. to obtain the title product. ¹H NMR (CHLOROFORM-d) δ: 7.50 - 7.64 (m, 4H), 4.65 (s, 2H), 4.21 (q, *J* = 7.02 Hz, 4H), 3.37 (s, 1H), 1.29 (t, *J* = 7.21 Hz, 6H).

4.4.2. 2-((5,7-dioxo-4,5,6,7-tetrahydropyrazolo[1,5-a]pyrimidin-6-yl)methyl)benzonitrile tributylamine salt (**7**): 1 g (3.63 mM) diethyl 2-(2-cyanobenzyl)malonate and 0.3 g (3.63 mM) 1H-pyrazol-3-amine was added 1.35 g (7.26 mM) tributylamine and heated to 170 °C for 6 h. It was cooled to room temperature and excess tri-*n*-butylamine decanted away from the solid product. The latter was triturated overnight with isohexane, filtered and dried under vacuum to give the title compound. ¹H NMR (400 MHz, DMSO-d₆) δ 8.34 (d, *J* = 1.00 Hz, 1H), 7.93 - 8.00 (m, 1H), 7.60 - 7.84 (m, 4H), 6.45 - 6.56 (m, 1H), 5.28 - 5.36 (m, 2H), 2.83 - 3.05 (m, 6H), 1.40 - 1.56 (m, 6H), 1.17 - 1.31 (m, 6H), 0.68 - 0.90 (m, 9H).

4.4.3. 2-((5,7-dichloropyrazolo[1,5-a]pyrimidin-6-yl)methyl)benzonitrile (**8**): Under nitrogen gas atmosphere, phosphorous oxychloride 30 (160 mL, 1.72 mol) and dimethylaniline (16 mL, 132 mmol) was added successively to the 2-((5,7-dioxo-4,5,6,7-tetrahydropyrazolo[1,5-a]pyrimidin-6-yl)methyl)benzonitrile tributylamine salt (16 g, 97 mmol). The mixture was heated at 110° C. for 4 hours then excess POC₁₃ was removed under vacuum. The residue was made basic with 3N NaOH solution (pH=9-10) and extracted with ethyl acetate (×3). The combined organic layers were dried over anhydrous Na₂SO₄, filtered, and concentrated under vacuum. The residue was purified by silica gel chromatography (100percent DCM) to provide 15.8 grams of the solid yellow product, (81% yield). ¹H NMR (400 MHz, DMSO-d₆) δ 8.26 (d, 1H), 7.77 (d, 1H), 7.66 (m, 2H), 7.52 (m, 2H), 5.34 (s, 2H).

4.4.4. (R)-2-((7-(3-aminopiperidin-1-yl)-5-chloropyrazolo[1,5-a]pyrimidin-6-yl)methyl)benzonitrile (**d1**): To a solution of 2-((5,7-dichloropyrazolo[1,5-a]pyrimidin-6-yl)methyl)benzonitrile in THF was add (R)-tert-butyl piperidin-3-ylcarbamate and TEA and stirred at ambient temperature overnight. The reaction was monitored by TLC. After the completion of the

reaction, the solvent was removed by vacuum and the crude product was purified by F.C.C. to obtain (R)-tert-butyl (1-(5-chloro-6-(2-cyanobenzyl)pyrazolo[1,5-a]pyrimidin-7-yl)piperidin-3-yl)carbamate. The product was put into DCM:TFA=20:1 solution and stirred at ambient temperature for 1h. After the completion of the reaction, DCM and 1N NaOH was added to the mixture, the organic layer was washed with water. Collect the organic layer and removed the solvent with vacuum. The crude product was purified by F.C.C. to obtain the title product (10% in two steps). m.p. = 138-140 °C; ¹H NMR (400 MHz, CHLOROFORM-d) δ 8.01 - 8.25 (m, 1H), 7.80 - 7.93 (m, 1H), 7.42 - 7.60 (m, 2H), 7.19 - 7.25 (m, 2H), 5.56 (m, 2H), 3.69 - 4.22 (m, 2H), 3.54 (d, *J* = 10.56 Hz, 1H), 2.83 (t, *J* = 7.43 Hz, 1H), 2.09 - 2.45 (m, 2H), 1.62 - 1.97 (m, 2H), 0.90 - 1.04 (m, 1H); ¹³C NMR (CHLOROFORM-d) δ: 161.5, 160.6, 158.8, 138.4, 137.6, 132.2, 131.4, 129.9, 126.4, 115.8, 113.3, 97.9, 83.5, 51.1, 46.7, 45.0, 44.1, 39.7, 29.6; HRMS (ESI): calcd for C₁₉H₂₀ClN₆ [M + H]⁺ 367.1438; found 367.1440.

4.5. IC₅₀ assays for DPP-4, DPP-8 and DPP-9

Solutions of test compounds in varying concentrations (≤10 mM final concentration) were prepared in dimethyl sulfoxide (DMSO) and then diluted into assay buffer comprising: 20 mM Tris, pH 7.4; 20 mM KCl; and 0.1 mg/mL BSA. Human DPP-4 (0.1 nM final concentration) was added to the dilutions and pre-incubated for 10 minutes at ambient temperature before the reaction was initiated with A-P-7-amido-4-trifluoromethylcoumarin (AP-AFC; 10 μM final concentration). The total volume of the reaction mixture was 100 μL depending on assay formats used (96 well plates). The reaction was followed kinetically (excitation λ= 400 nm; emission λ= 505 nm) for 5-10 minutes or an end-point was measured after 10 minutes. Inhibition constants (IC₅₀) were calculated from the enzyme progress curves using standard mathematical models¹⁶.

Recombinant human DPP-8 and DPP-9 (X-Y biotechnology, Shanghai, China) were diluted to a final volume of 50 μL in assay buffer (100 mM Tris-HCl, 100 mM NaCl, pH 7.8) and added to 96-well flat-bottom microtiter plates, followed by the addition of 10 μL inhibitor and 40 μL substrate (H-Gly-Pro-AMC, GL Biochem(Shanghai)Ltd., final concentration in the assay, 303 μM). The plates were incubated at 37°C for 10 min. after incubation, fluorescence was measured using microplate reader (excitation 380 nm/ emission 460 nm)²⁹.

4.6. Cell cytotoxicity MTT assay

This experiment was carried out on a 96-well plate. HepG2 cells in 100 μL DMEM were incubated with the negative control (1 μL of DMSO) or the inhibitors (dissolved in DMSO) at doses ranging from 1 μM to 100 μM (final concentration) for 48 hrs. Then 20 μL of 5 mg/ml MTT was added to the mixture followed by a 6 h-incubation. After the incubation, the upper clear solution was carefully removed followed by the addition of 100 μL of DMSO. The plate was shaken gently for 1 min so that complete dissolution was achieved. The absorbance of the solution at 490 nm was measured using the microplate spectrophotometer system (Thermo Scientific

Varioskan Flash). Cell viability was calculated based on the OD values.

Acknowledgments

We thank the Medicine and Engineering interdisciplinary Research Fund of Shanghai Jiao Tong University (YG2015QN03, YG2014MS10 and YG2017MS77), National Natural Science Foundation of China (81202397) and Shanghai Natural Science Fund (12ZR1415400) for the financial support. We thank Professor Yongxiang Wang's Laboratory (Shanghai Jiao Tong University) for the biological support of this research.

References

1. S. Chatterjee, K. Khunti, M.J. Davies. Type 2 diabetes. *Lancet*. 2017; 389: 2239-2251.
2. T.M. Barber, H. Begbie, J. Levy. The incretin pathway as a new therapeutic target for obesity. *Maturitas*. 2010; 67: 197-202.
3. M.B. Toft-Nielsen, S. Madsbad, J.J. Holst. Determinants of the effectiveness of glucagon-like peptide-1 in type 2 diabetes. *J Clin Endocrinol Metab*. 2001; 86: 3853-3860.
4. T.J. Kieffer, C.H. McIntosh, R.A. Pederson. Degradation of glucose-dependent insulinotropic polypeptide and truncated glucagon-like peptide 1 in vitro and in vivo by dipeptidyl peptidase IV. *Endocrinology*. 1995; 136: 3585-3596.
5. J.A. Pospisilik, S.G. Stafford, H.U. Demuth, R. Brownsey, W. Parkhouse, D.T. Finegood, C.H. McIntosh, R.A. Pederson. Long-term treatment with the dipeptidyl peptidase IV inhibitor P32/98 causes sustained improvements in glucose tolerance, insulin sensitivity, hyperinsulinemia, and beta-cell glucose responsiveness in VDF (fa/fa) Zucker rats. *Diabetes*. 2002; 51: 943-950.
6. Y. Li, Medicine used for treating alopecia and leukotrichia, comprises lithium chloride, 4-(6-(4-(piperazin-1-yl)phenyl)pyrazolo(1,5-a)pyrimidin-3-yl)quinoline hydrochloride, and carrier or excipient, CN106727682-A, 2017; 9.
7. K. Niazi, S. Rabizadeh, A. Leny, O. Buzko, J. Golovato, P. Soon-Shiong, Pharmaceutical composition useful for reducing viral propagation e.g. Marburg virus, comprises 2-phenyl-pyrazolo(1,5-a)pyrimidin-7-ylamine derivative in combination with carrier, US2017128450-A1, 2017; 20.
8. B.K. Albrecht, S.F. Bellon, V.S. Gehling, J.-C. Harmange, Y. LeBlanc, J. Liang, S.R. Magnuson, V.H.-W. Tsui, B. Zhang, Pyrazolo 1,5-A pyrimidin-7(4H)-one/histone demethylase inhibitors, US 09505767, 2016.
9. Y. Sheng, B. Sun, W.T. Guo, X. Liu, Y.C. Wang, X. Xie, X.L. Xiao, N. Li, D.L. Dong. (4-[6-(4-isopropoxyphenyl)pyrazolo [1,5-a]pyrimidin-3-yl] quinoline) is a novel inhibitor of autophagy. *Br J Pharmacol*. 2014; 171: 4970-4980.
10. M.A. El-Gahami, A.E. Mekky, T.S. Saleh, A.S. Al-Bogami. Acidity constant and solvatochromic behavior of some pyrazolo[1,5-a]pyrimidin-2-amine derivatives. *Spectrochim Acta A Mol Biomol Spectrosc*. 2014; 129: 209-218.
11. Y. Sheng, B. Sun, X. Xie, N. Li, D. Dong. DMH1 (4-[6-(4-isopropoxyphenyl)pyrazolo[1,5-a]pyrimidin-3-yl]quinoline) inhibits chemotherapeutic drug-induced autophagy. *Acta Pharm Sin B*. 2015; 5: 330-336.
12. D. Tang, M.L. Nickels, M.N. Tantawy, J.R. Buck, H.C. Manning. Preclinical imaging evaluation of novel TSPO-PET ligand 2-(5,7-Diethyl-2-(4-(2-[(18)F]fluoroethoxy)phenyl)pyrazolo[1,5-a]pyrimidin-3-yl)-N,N-diethylacetamide ([(18)F]VUIIS1008) in glioma. *Mol Imaging Biol*. 2014; 16: 813-820.
13. G. Guerrini, G. Ciciani, S. Daniele, C.M.L. Di, C. Ghelardini, C. Martini, S. Selleri. Synthesis and pharmacological evaluation of pyrazolo[1,5-a]pyrimidin-7(4H)-one derivatives as potential GABAA-R ligands. *Bioorg Med Chem*. 2017; 25: 1901-1906.
14. Y. Ikuma, H. Hochigai, H. Kimura, N. Nunami, T. Kobayashi, K. Uchiyama, Y. Furuta, M. Sakai, M. Horiguchi, Y. Masui, K. Okazaki, Y. Sato, H. Nakahira. Discovery of 3H-imidazo[4,5-c]quinolin-4(5H)-ones as potent and selective dipeptidyl peptidase IV (DPP-4) inhibitors. *Bioorg Med Chem*. 2012; 20: 5864-5883.
15. Z. Zhang, M.B. Wallace, J. Feng, J.A. Stafford, R.J. Skene, L. Shi, B. Lee, K. Aertgeerts, A. Jennings, R. Xu, D.B. Kassel, S.W. Kaldor, M. Navre, D.R. Webb, S.L. Gwaltney. Design and synthesis of pyrimidinone and pyrimidinedione inhibitors of dipeptidyl peptidase IV. *J Med Chem*. 2011; 54: 510-524.

16. J. Feng, Z. Zhang, M.B. Wallace, J.A. Stafford, S.W. Kaldor, D.B. Kassel, M. Navre, L. Shi, R.J. Skene, T. Asakawa, K. Takeuchi, R. Xu, D.R. Webb, S.L. Gwaltney, 2nd. Discovery of alogliptin: a potent, selective, bioavailable, and efficacious inhibitor of dipeptidyl peptidase IV. *J Med Chem*. 2007; 50: 2297-2300.
17. S. Li, H. Xu, S. Cui, F. Wu, Y. Zhang, M. Su, Y. Gong, S. Qiu, Q. Jiao, C. Qin, J. Shan, M. Zhang, J. Wang, Q. Yin, M. Xu, X. Liu, R. Wang, L. Zhu, J. Li, Y. Xu, H. Jiang, Z. Zhao, J. Li, H. Li. Discovery and Rational Design of Natural-Product-Derived 2-Phenyl-3,4-dihydro-2H-benzo[f]chromen-3-amine Analogs as Novel and Potent Dipeptidyl Peptidase 4 (DPP-4) Inhibitors for the Treatment of Type 2 Diabetes. *J Med Chem*. 2016; 59: 6772-6790.
18. C. Schwehm, J. Li, H. Song, X. Hu, B. Kellam, M.J. Stocks. Synthesis of New DPP-4 Inhibitors Based on a Novel Tricyclic Scaffold. *ACS Med Chem Lett*. 2015; 6: 324-328.
19. Y. Ran, H. Pei, M. Shao, L. Chen. Synthesis, Biological Evaluation, and Molecular Docking of (R)-2-((8-(3-aminopiperidin-1-yl)-3-methyl-7-(3-methylbut-2-en-1-yl)-2,6-dioxo-2,3,6,7-tetrahydro-1H-purin-1-yl)methyl)benzotrile as Dipeptidyl Peptidase IV Inhibitors. *Chem Biol Drug Des*. 2016; 87: 290-295.
20. J.M. Cox, H.D. Chu, J.T. Kuethe, Y.D. Gao, G. Scapin, G. Eiermann, H. He, X. Li, K.A. Lyons, J. Metzger, A. Petrov, J.K. Wu, S. Xu, R. Sinha-Roy, A.E. Weber, T. Biftu. The discovery of novel 5,6,5- and 5,5,6-tricyclic pyrrolidines as potent and selective DPP-4 inhibitors. *Bioorg Med Chem Lett*. 2016; 26: 2622-2626.
21. C. Shu, H. Ge, M. Song, J.H. Chen, H. Zhou, Q. Qi, F. Wang, X. Ma, X. Yang, G. Zhang, Y. Ding, D. Zhou, P. Peng, C.K. Shih, J. Xu, F. Wu. Discovery of imigliptin, a Novel Selective DPP-4 Inhibitor for the Treatment of Type 2 Diabetes. *ACS Med Chem Lett*. 2014; 5: 921-926.
22. H. Xie, L. Zeng, S. Zeng, X. Lu, X. Zhao, G. Zhang, Z. Tu, H. Xu, L. Yang, X. Zhang, S. Wang, W. Hu. Highly potent dipeptidyl peptidase IV inhibitors derived from Alogliptin through pharmacophore hybridization and lead optimization. *Eur J Med Chem*. 2013; 68: 312-320.
23. Q. Li, L. Han, B. Zhang, J. Zhou, H. Zhang. Synthesis and biological evaluation of triazole based uracil derivatives as novel DPP-4 inhibitors. *Org Biomol Chem*. 2016; 14: 9598-9611.
24. Y. Ikuma, H. Hochigai, H. Kimura, N. Nunami, T. Kobayashi, K. Uchiyama, T. Umezome, Y. Sakurai, N. Sawada, J. Tadano, E. Sugaru, M. Ono, Y. Hirose, H. Nakahira. Discovery of 3H-imidazo[4,5-c]quinolin-4(5H)-ones as potent and selective dipeptidyl peptidase IV (DPP-4) inhibitors: use of a carboxylate prodrug to improve bioavailability. *Bioorg Med Chem*. 2015; 23: 779-790.
25. W.L. Wu, J. Hao, M. Domalski, D.A. Burnett, D. Pissarnitski, Z. Zhao, A. Stamford, G. Scapin, Y.D. Gao, A. Soriano, T.M. Kelly, Z. Yao, M.A. Powles, S. Chen, H. Mei, J. Hwa. Discovery of Novel Tricyclic Heterocycles as Potent and Selective DPP-4 Inhibitors for the Treatment of Type 2 Diabetes. *ACS Med Chem Lett*. 2016; 7: 498-501.
26. P.F. Xiao, R. Guo, S.Q. Huang, H.J. Cui, S. Ye, Z.Y. Zhang. Discovery of dipeptidyl peptidase IV (DPP4) inhibitors based on a novel indole scaffold. *Chin Chem Lett*. 2014; 25: 673-676.
27. K. Namoto, F. Sirockin, N. Ostermann, F. Gessier, S. Flohr, R. Sedrani, B. Gerhartz, J. Trappe, U. Hassiepen, A. Duttaroy, S. Ferreira, J.M. Sutton, D.E. Clark, G. Fenton, M. Beswick, D.K. Baeschlin. Discovery of C-(1-aryl-cyclohexyl)-methylamines as selective, orally available inhibitors of dipeptidyl peptidase IV. *Bioorg Med Chem Lett*. 2014; 24: 731-736.
28. K. Jansen, L. Heirbaut, J.D. Cheng, J. Joossens, O. Ryabtsova, P. Cos, L. Maes, A.M. Lambeir, I. De Meester, K. Augustyns, P. Van der Veken. Selective Inhibitors of Fibroblast Activation Protein (FAP) with a (4-Quinolinoyl)-glycyl-2-cyanopyrrolidine Scaffold. *ACS Med Chem Lett*. 2013; 4: 491-496.
29. H. Xie, L. Zeng, S. Zeng, X. Lu, G. Zhang, X. Zhao, N. Cheng, Z. Tu, Z. Li, H. Xu, L. Yang, X. Zhang, M. Huang, J. Zhao, W. Hu. Novel pyrrolopyrimidine analogues as potent dipeptidyl peptidase IV inhibitors based on pharmacokinetic property-driven optimization. *Eur J Med Chem*. 2012; 52: 205-212.

